Vision Research 107 (2015) 1–14

Contents lists available at ScienceDirect

Vision Research

journal homepage: www.elsevier.com/locate/visres

The influence of crystalline lens accommodation on post-saccadic oscillations in pupil-based eye trackers

Marcus Nyström [a,*], Richard Andersson [a], Måns Magnusson [b], Tony Pansell [c,d], Ignace Hooge [e]

[a] Humanities Laboratory, Lund University, Helgonabacken 12, 22362 Lund, Sweden
[b] Department of Otorhinolaryngology Head and Neck Surgery, Clinical Sciences, Lund University, Lund, Sweden
[c] St. Erik Eye Hospital, Stockholm, Sweden
[d] Department of Clinical Neuroscience, Karolinska Institutet, Stockholm, Sweden
[e] Experimental Psychology, Helmholtz Institute, Utrecht University, Utrecht, The Netherlands

ARTICLE INFO

Article history:
Received 25 June 2014
Received in revised form 13 October 2014
Available online 4 December 2014

Keywords:
Eye tracking
Post-saccadic oscillation
Pupil
Lens
Accommodation

ABSTRACT

It is well known that the crystalline lens (henceforth lens) can oscillate (or 'wobble') relative to the eyeball at the end of saccades. Recent research has proposed that such wobbling of the lens is a source of post-saccadic oscillations (PSOs) seen in data recorded by eye trackers that estimate gaze direction from the location of the pupil. Since the size of the lens wobbles increases with accommodative effort, one would predict a similar increase of PSO-amplitude in data recorded with a pupil based eye tracker. In four experiments, we investigated the role of lens accommodation on PSOs in a video-based eye tracker. In Experiment 1, we replicated previous results showing that PSO-amplitudes increase at near viewing distances (large vergence angles), when the lens is highly accommodated. In Experiment 2a, we manipulated the accommodative state of the lens pharmacologically using eye drops at a fixed viewing distance and found, in contrast to Experiment 1, no significant difference in PSO-amplitude related to the accommodative state of the lens. Finally, in Experiment 2b, the effect of vergence angle was investigated by comparing PSO-amplitudes at near and far while maintaining a fixed lens accommodation. Despite the pharmacologically fixed degree of accommodation, PSO-amplitudes were systematically larger in the near condition. In summary, PSOs cannot exhaustively be explained by lens wobbles. Possible confounds related to pupil size and eye-camera angle are investigated in Experiments 3 and 4, and alternative mechanisms behind PSOs are probed in the discussion.

1. Introduction

Post-saccadic oscillations (PSOs) refer to the period of instability that can be observed in an eye tracker signal immediately following a saccade (see Fig. 1) (Larsson, Nyström & Stridh, 2013; Nyström, Hooge & Holmqyist, 2013). There are at least three important reasons to investigate PSOs. First, they complicate the decision of where a saccade should end and consequently where the next fixation should begin. This uncertainty is transferred to higher order measures using fixation and saccades, such as average fixation or saccade duration. Second, oscillations of different ocular structures may have important perceptual implications (Deubel & Bridgeman, 1995a, 1995b). Third, PSOs can originate from different sources, which makes it difficult to separate neurologically deviating oscillations caused by disorders such as the Niemann–Pick type C disease (Leigh & Zee, 2006, p. 114) from those that originate from other sources, e.g., dynamic overshoot (Kapoula, Robinson & Hain, 1986). The prevalence of PSOs largely depends on individual factors and the principle used to record the eye movements (Nyström, Hooge & Holmqyist, 2013). PSOs are particularly large (up to five degrees) in data recorded by Dual Purkinje Image (DPI) eye trackers (Crane & Steele, 1985; Deubel & Bridgeman, 1995a) measuring lens movement, but typically small (<0.2 deg.) in data recorded with scleral search coils, which measure eyeball rotation (Kapoula, Robinson & Hain, 1986). This has been explained by the fact that the lens moves inside the eyeball during and directly after saccades (Deubel & Bridgeman, 1995a).

Despite being known for their high accuracy and precision, scleral search coils and DPIs are being replaced by simpler-to-use video-based systems estimating the gaze direction from the pupil and corneal reflections (CRs) in the video image of the eye. The underlying assumption of pupil-based eye trackers is that the pupil movement is a good estimate of the eyeball rotation. Interestingly,

* Corresponding author.
E-mail addresses: marcus.nystrom@humlab.lu.se (M. Nyström), richard.andersson@humlab.lu.se (R. Andersson), mans.magnusson@med.lu.se (M. Magnusson), tony.pansell@ki.se (T. Pansell), i.hooge@uu.nl (I. Hooge).

http://dx.doi.org/10.1016/j.visres.2014.10.037
0042-6989/

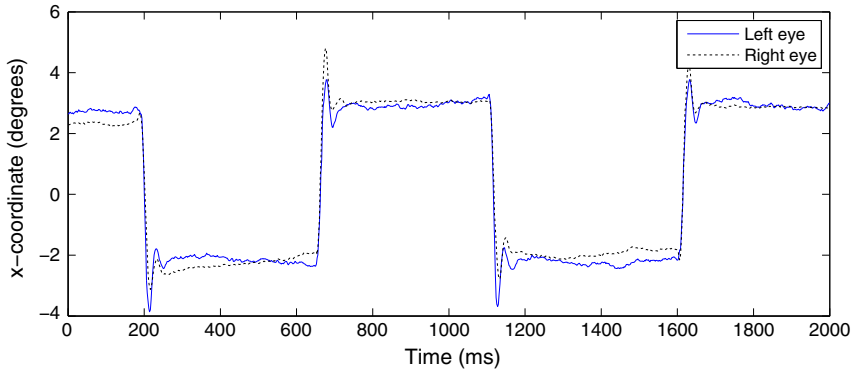

Fig. 1. Saccades and post-saccadic oscillations (PSOs) recorded with a pupil based eye tracker (the iView X Hi-Speed system from SensoMotoric Instruments) at 500 Hz using default settings. Data were collected from a participant who conducted horizontal, five degree saccades. No additional processing has been applied to the data after the recording.

PSOs also appear in high-end pupil based eye trackers such as the EyeLink 1000 from SR-Research and the iView X Hi-speed system from SensoMotoric Instruments (SMI).

Even though their appearance in the data has been long known, the origin of PSOs in pupil-based eye tracker has recently caught significant interest in parts of the eye movement community (Kimmel, Mammo and Newsome, 2012; Nyström, Hooge and Holmqyist, 2013; Hooge et al., 2013; Hutton, 2013). Kimmel, Mammo and Newsome (2012) compared data from surgically implanted coils in monkeys with simultaneous recording from an EyeLink 1000 and reported significantly more and larger PSOs in the EyeLink data. They argue that the PSOs may be a result of the fact that the systems measure different ocular structures, with the pupil moving relative to the whole eyeball. Recent findings by Nyström, Hooge and Holmqyist (2013) verified this prediction by measuring the discrepancy between the motion of the pupil and the iris (estimating eyeball motion) immediately preceding and following the end of a saccade; the pupil center oscillated with a higher frequency and a larger amplitude than the iris center.

While the findings by Nyström, Hooge and Holmqyist (2013) explain why we see PSOs in the data, they do not reveal the physiological model of the oscillations. Given that the lens wobbles directly after saccades, and the direct proximity between the lens and the pupil (see Fig. 2), one could hypothesize that the pupil oscillations are direct consequences of the lens wobble. There are both theoretical predictions and ample empirical evidence that the accommodative state of the lens influences the amplitude of lens wobbles following saccades. According to Helmholtz's theory of accommodation, decreased zonular tension leads to higher instability of the lens during accommodation (Glasser & Kaufman, 1999). During saccadic eye movements this theory predicts a higher peak velocity and larger post-saccadic oscillations of the lens during accommodation, which is in line with empirical results by Deubel and Bridgeman (1995a) and He et al. (2010). Given a causal link between movements of the lens and the pupil, one would predict the same general pattern for the pupil oscillations. This prediction was supported empirically by Hutton (2013), who reported that PSOs recorded with an EyeLink 1000 increased at near accommodation with respect to duration and amplitude as well as the number of oscillations and the proportion of saccades showing PSOs. These findings were interpreted as if lens wobble is a source of PSOs in pupil-based eye trackers.

The close proximity between the lens and pupil, as well as the empirical findings by Hutton (2013) led us to hypothesize that lens wobble is the main source of PSOs in pupil-based eye trackers. The overarching aim of this paper is to test this hypothesis, which we refer to as the *lens–pupil* hypothesis. This will be done by further investigating the role of the crystalline lens and its accommodation on PSOs in pupil-based eye trackers. In Experiment 1, we use the SMI Hi-speed system to replicate Hutton's experiment, where properties of PSOs are quantified at different viewing distances (i.e., degrees of accommodation). In Experiment 2a, to avoid the possible confound of vergence angle, lens accommodation is manipulated pharmacologically to induce a maximum and minimum degree of accommodation while keeping the viewing distance fixed. In both experiment 1 and 2a we predict according to the lens–pupil hypothesis that the maximally accommodated lens will produce larger saccade peak velocity and larger PSOs than the minimally accommodated lens. In Experiment 2b we compare PSOs at near and far after pharmacological manipulation of lens accommodation. Since the lens is either maximally or minimally accommodated irrespective of vergence angle, we do, according to the lens–pupil hypothesis, expect no or small difference in PSO size.

To probe additional mechanisms behind PSOs, Experiments 3 and 4 are conducted to investigate the influence of pupil size and eye orientation relative to the eye-tracker camera on PSOs. A summary of the experiments and their manipulations is provided in

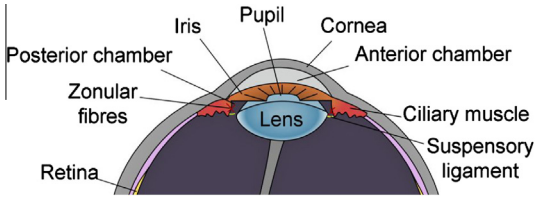

Fig. 2. An intersection of the human eye showing the close spatial proximity between the lens and the iris. Is there a mechanical coupling strong enough to cause the iris and therefore the pupil to oscillate during high acceleration saccades? Adapted from Wikimedia commons.

Table 1
Overview of the experimental manipulations showing the independent variables (IV), the manipulations, and whether the vergence angle and/or the degree of lens accommodation are controlled for.

	IV	Manipulation	Controlled for
Exp. 1	Accom. (high/low)	Viewing dist.	–
Exp. 2a	Accom. (high/low)	Eye drops	Vergence
Exp. 2b	Vergence (high/low)	Viewing dist.	Accom.
Exp. 3	Pupil size (large/small)	Brightness	Vergence/ Accom.
Exp. 4	Gaze direction (−10, 0, 10 deg.)	Eye orientation	Vergence/ Accom.

Table 1. All experiments were conducted in accordance with the Declaration of Helsinki, and informed consent was obtained for experimentation with human subjects.

2. Experiment 1

2.1. Participants

Four people (three of the authors) participated in the study: MN (age: 35 years, gender: m), RA (34/m), IH (47/m), TC (25/m).

2.2. Stimulus

The stimulus consisted of two 0.2 deg. white dots presented on a black background. The dots were separated by five degrees horizontally and were aligned vertically. Their center of gravity coincided with the center of the screen.

2.3. Apparatus

Binocular eye movements were recorded at 500 Hz with the Hi-speed system from SensoMotoric Instruments (Berlin, Germany) using iView X v. 2.7.13 with default settings. Besides gaze direction and pupil size, this system records the position of the first Purkinje reflection (P_1) in the eye image. The P_1 is the result of incoming IR-light reflected off the front surface of the cornea, and therefore moves with the translation and rotation of the eyeball. Only data from the left eye were analyzed and reported. The stimulus was shown on a Samsung Syncmaster 60 Hz LCD monitor with resolution 1280 × 1024 pixels (380 × 300 mm) using Matlab v. 7.11.0, R2010b and the Psychophysics Toolbox v. 3.0.9, rev. 2450.

2.4. Procedure

The participants were positioned such that the center of screen was aligned vertically with the center of the eyes and horizontally with the nose.

Eye movements were recorded at two different viewing distances: near (17 cm) and far (70 cm). These distances were similar to values used in earlier studies reporting changes in eye movements due to accommodation (Deubel and Bridgeman, 1995a; Schachar et al., 2007; He et al., 2010; Hutton, 2013). In our case, 17 cm was the closest viewing distance allowed by the physical setup.

Participants were instructed to conduct two saccades per second between the stimulus dots during 60 s in each of the two conditions (near/far). A recording was preceded by a 13-point calibration covering an area of 20 × 10 deg. The center of the calibration area was aligned with the center of the screen.

2.5. Data analysis

Saccade candidates were detected by the algorithm from Engbert and Kliegl (2003) with a minimum saccade duration of 16 ms (eight samples) and $\lambda = 4$. Since PSOs complicate the decision of where a saccade should end, we have chosen to compute saccade amplitudes from 'saturated' values, i.e., when the signal reaches a stable x-value before and after the actual saccade. The position of the saccade onset was computed as the median x-value of 30 samples preceding the onset of the saccade candidate. Similarly, the saccade offset position was the median of 30 samples following the PSO offset, as computed below. Saccade peak velocity was taken as the largest velocity sample during the saccade.

Only horizontal saccades (<1 deg. vertical extent) with amplitudes within 0.5 deg. of the target amplitude (5 deg.) were included in the analysis. The amplitude of a PSO following a saccade that passed this test was computed as follows:

1. A line was robustly fit[1] to four points within a sliding window, starting at the saccade peak velocity and ending 90 samples after the end of the saccade.
2. The PSO started at the first location when the slope of the line exceeded −0.02 deg./s.
3. Finally, the PSO amplitude was computed as the difference between the y-coordinate at PSO onset and the first y-coordinate after PSO onset where slope of the fitted line went below 0.02 deg./s.

Since this procedure is designed for leftward saccades, rightward saccades were 'flipped' before being included in the analysis.

Differences between viewing conditions and pharmacological treatments were tested statistically in R v. 3.0.2 (R Core Team, 2013) using linear mixed effect models (Bates et al., 2013) with random factors for modeling the participant-level intercepts and slopes. Differences within participants across viewing conditions were tested statistically using paired t-tests. PSO-amplitudes were square-root transformed to approach a Gaussian-like distribution before being used in the statistical tests. A t-value $|t| > 2$ or a p-value $p < 0.01$ were considered to be statistically significant.

Finally, to investigate the contribution of overshoot from the whole eye globe on PSOs, the P_1 was extracted from the eye tracker data. Since the P_1-signal is not calibrated and mapped to spatial coordinates on the screen, the PSO-amplitude of the P_1-signal in degrees is estimated by multiplying its amplitude in camera pixels with the quotient of the saccade amplitude in degrees and the amplitude of the saccade in camera pixels. The amplitude of the latter was computed from 'saturated' values in the P_1-signal, as described above.

Table 2
Summary of saccade properties. Part. – initials of participants; Cond. – near (N) or far (F); No. – number of saccades; PV – saccade peak velocity in deg./s; A_{PSO} – PSO amplitude; $A_{PSO}^{P_1}$ – PSO amplitude of P_1.

Part.	Cond.	No.	PV (M ± SD)	A_{PSO} (M ± SD)	$A_{PSO}^{P_1}$ (M ± SD)
IH	N	45	376.50 ± 63.84	1.51 ± 0.58	0.15 ± 0.11
IH	F	58	318.11 ± 28.71	0.60 ± 0.24	0.09 ± 0.06
TC	N	63	320.42 ± 30.21	0.96 ± 0.22	0.18 ± 0.15
TC	F	47	270.61 ± 24.14	0.23 ± 0.22	0.16 ± 0.12
RA	N	46	435.44 ± 61.70	2.34 ± 0.50	0.23 ± 0.16
RA	F	57	317.48 ± 36.33	0.33 ± 0.19	0.11 ± 0.09
MN	N	93	453.45 ± 75.59	1.79 ± 0.64	0.38 ± 0.28
MN	F	90	370.35 ± 50.71	1.31 ± 0.38	0.20 ± 0.15

2.6. Results

General properties of the detected saccades are given in Table 2. Overall, saccade peak velocities were about 23% higher at near compared to far (near 402.14 ± 82.62 deg./s, far: 327.7 6 ± 52.99 deg./s, $t > 2$, cf. Table 3). Moreover, significant differences in saccade peak velocities were found when analyzing saccades within each participant separately (all with larger saccade peak velocity at near, $p < 0.01$ using paired t-tests).

Fig. 3 shows data from one participant performing five-degree leftward saccades at near (a) and far (b) viewing distances. As can be seen from the figure, there is a large difference in PSO-amplitude and dynamics in the two conditions; PSOs at near have

[1] using `robustfit` in Matlab. See http://www.mathworks.se/help/stats/robustfit.html for details.

Table 3
Results of the linear mixed effect model when predicting **saccade peak velocity** from viewing condition (near and far). The table shows that velocities in the near condition are significantly larger ($t > 2$) than those in the far condition. Significance is indicated by '*'. Notice that the saccade peak velocities are log transformed before being used in the model.

	Estimate	Std. error	*t* value
(Intercept)	5.75	0.06	91.02
Near	0.21	0.03	5.97*

considerably longer durations and larger amplitudes than those from equally sized saccades at far.

Fig. 4 presents the difference in PSO-amplitude between near and far for all participants. The results are given separately for leftward and rightward saccades. Most importantly, it can been seen that the difference between the two conditions in terms of PSO-amplitude generalizes to all four participants, irrespective of the saccade direction. On average, the PSO-amplitude increased by 126% at near compared to far. This difference was significant (near:

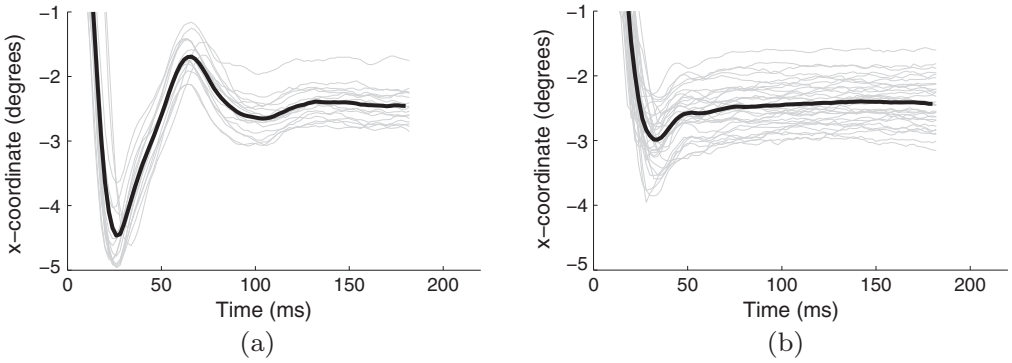

Fig. 3. PSO-trajectories for five-degree saccades at two viewing distances: (a) 17 cm and (b) 70 cm. The data show leftward saccades performed by participant RA, who showed the largest difference between near and far. The gray lines represent data from individual saccades and the black line corresponds to the average signal. All saccades started from the *x*-coordinate 2.5 deg. and are plotted from the point of the saccade peak velocity.

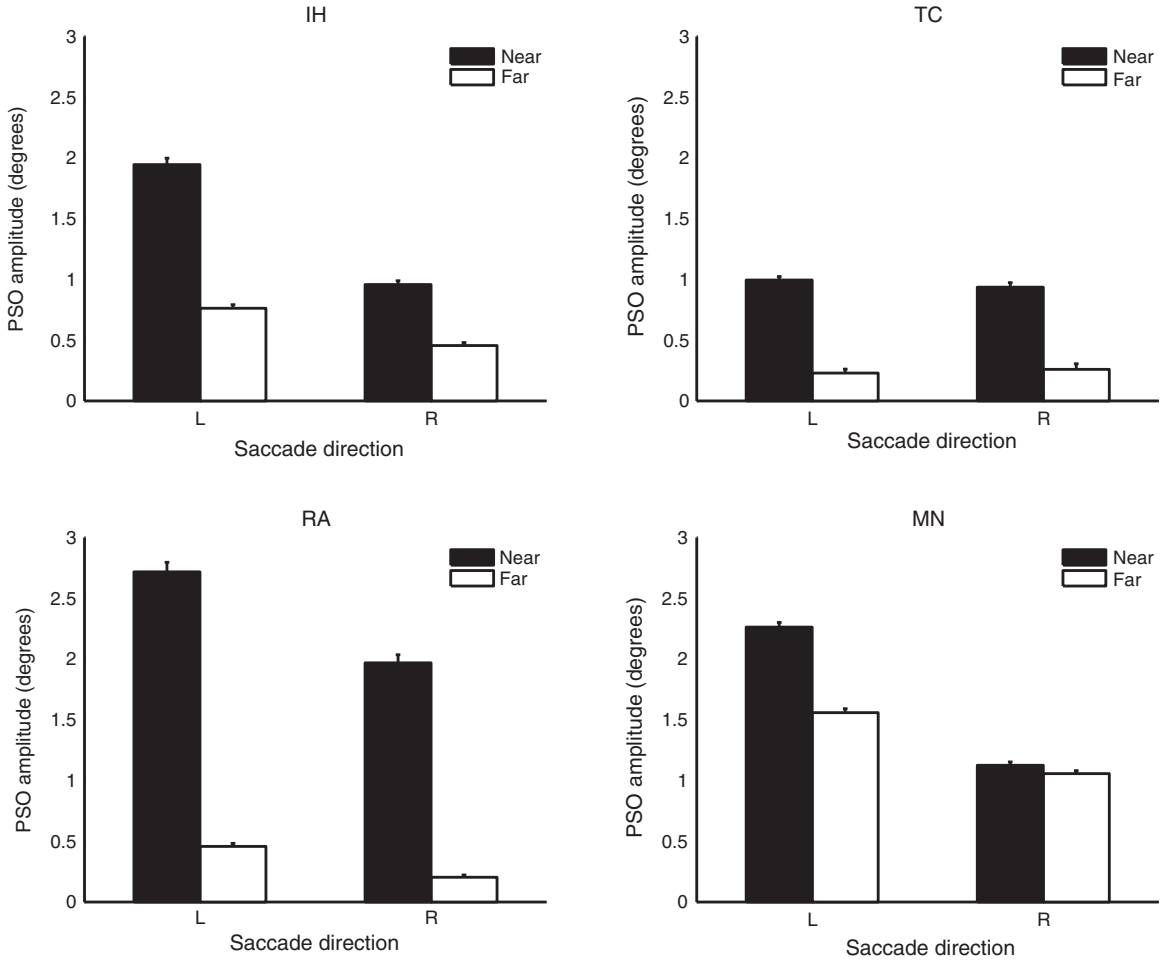

Fig. 4. Amplitudes of PSOs for each viewing condition (near/far) and saccade direction (left/right). Error bars represent standard errors of the mean.

Table 4
Results of the linear mixed-effects model when predicting **PSO-amplitude** from viewing condition (near and far) and saccade direction (adducting and abducting). The table shows that PSO-amplitudes in the near condition are significantly larger than those in the far condition, and that abducting saccades are significantly larger than adducting saccades. Notice that the amplitudes are square-root transformed before being used in the model. Significance is indicated by '*'.

	Estimate	Std. error	*t* value
(Intercept)	0.80	0.17	4.78
Near	0.59	0.16	3.80*
Adducting	−0.18	0.05	−3.30*
Near:adducting	−0.12	0.07	−1.87

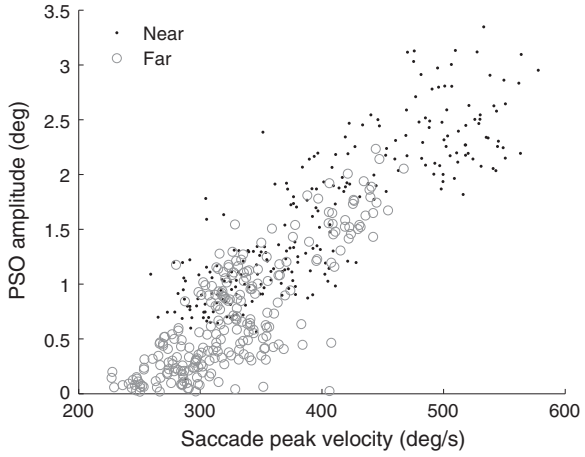

Fig. 5. Relationship between saccade peak velocity and PSO-amplitude for five degree saccades. Each dot represents a saccade/PSO pair from all saccades and participants.

1.63 ± 0.70, far: 0.72 ± 0.54, cf. Table 4). As with saccade peak velocities, there were significant differences in PSO-size also when participants were analyzed separately (all $p < 0.01$).

In agreement with previous work, there is a large individual variation in PSO-amplitude across participants (Nyström, Hooge & Holmqyist, 2013). It can also be observed that the PSO-amplitude can vary for the same person depending on the direction of the saccade, typically such that PSOs following abducting saccades have

Table 5
Results of the linear mixed-effects model when predicting **PSO-amplitude of the P_1-signal** from viewing condition (near and far). The table shows that PSO-amplitudes in the near condition were significantly larger than those in the far condition. Notice that the amplitudes were square-root transformed before being used in the model. Significance is indicated by '*'.

	Estimate	Std. error	*t* value
(Intercept)	0.34	0.03	10.94
Near	0.10	0.03	3.38*

larger amplitudes (cf. Table 4). Similar finding have been reported in data recorded from both scleral search coils (Kapoula, Robinson & Hain, 1986) and DPIs (Deubel & Bridgeman, 1995a).

As can be seen in Fig. 5, there was a high and significant Pearson-correlation between saccade peak velocity and PSO amplitude, both at near ($r = 0.86$, $p < 0.01$) and far ($r = 0.81$, $p < 0.01$). In the remainder of this paper, we therefore omit saccade peak velocity from further statistical analysis, and focus only on PSO-amplitudes.

Finally, as illustrated in Fig. 6, the differences between near and far in the P_1 signal were relatively small compared to the differences observed in the gaze coordinate signal, even though they originate from the same underlying saccade. On average, the PSO amplitude of the P_1-signal increased significantly at near compared to far (near: 0.26 ± 0.22, far: 0.14 ± 0.13, cf. Table 5).

2.7. Discussion

In summary, we found that both the saccade peak velocity and the PSO-amplitude increased at near compared to far viewing distances. These results are in line with the findings by Hutton (2013) as well as the hypothesis that post-saccadic wobbling of the lens is a source of PSOs in pupil-based eye trackers. By measuring the P_1, it was found that oscillations of the whole eye globe also increase significantly in the near condition. Importantly, the PSO-amplitude in the gaze-coordinate-signal was higher by more than a factor five than the amplitude of the P_1-oscillations. However, since a change in viewing distance affects other parameters than the lens accommodation, most importantly the vergence angle, we investigate in Experiment 2a whether the effect of PSO-amplitude can be replicated when lens accommodation is manipulated pharmacologically at a fixed viewing distance.

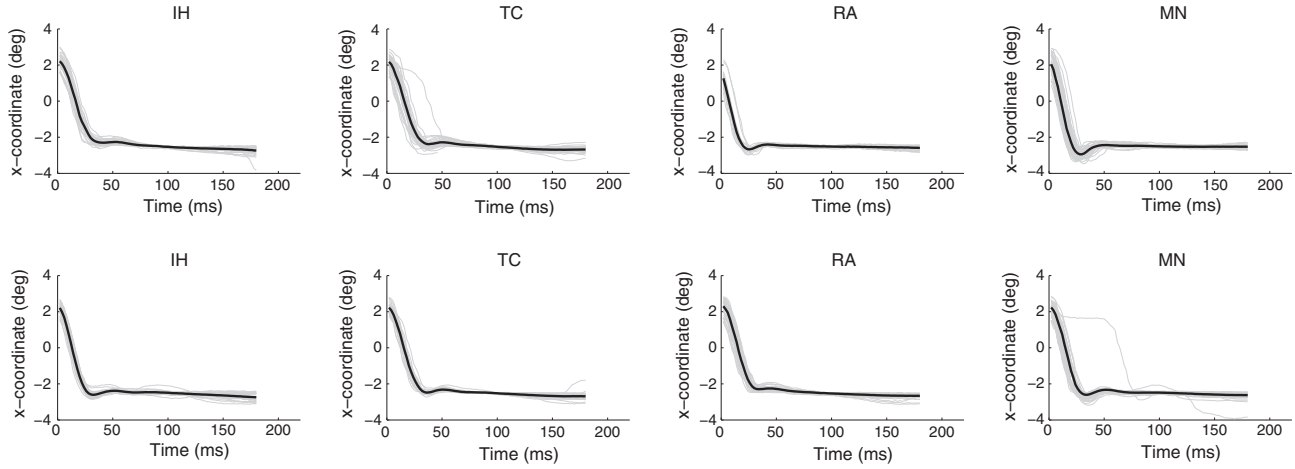

Fig. 6. The first Purkinje image (P_1)-signal at near (upper panel) and far (lower panel) viewing conditions. The signals originate from leftward saccades. To facilitate comparisons between the figures, the signals have been converted to degrees and centered around zero on the *y*-axis. Zero on the *x*-axis corresponds to the onset of the saccade candidate detected with the algorithm by Engbert and Kliegl (2003).

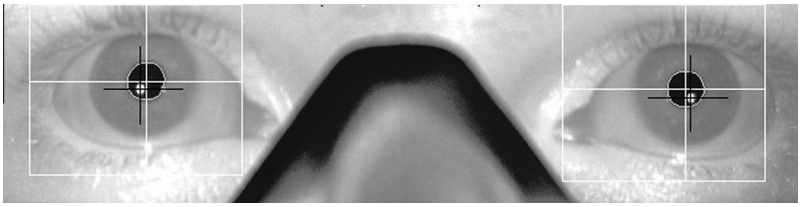

Fig. 7. Eye image captured with the SMI Hi-speed system.

3. Experiment 2a

3.1. Participants, materials, and procedure

The same participants, apparatus, and stimulus were used as in the first experiment. The degree of lens accommodation was manipulated pharmacologically by one drop of Cyclopentolat 1% (minimizes the accommodation) or Isopto-Pilokarpin 2% (maximizes the accommodation). A detailed description of how these substances affect the eye structures is provided in Rang et al. (2003, p. 144). To maximize the effect of the eye drops, the recording started 30 min after applying them to a participant. A full experiment lasted less than one hour. Participants viewed the stimulus at a fixed viewing distance of 70 cm in two conditions: with pharmacologically induced minimum and maximum accommodation. Only the participants' left eyes were manipulated. Moreover, since the effect of Cyclopentolat could last for up to 24 h, the recordings for a participants were conducted on different days, but always within three days.

After the saccade experiment was complete, participants were asked to fixate a centrally located target for one second, during which eye images were recorded. The eye images were collected at 500 Hz and saved as grayscale `JPEG` images with a resolution of 640 × 160 pixels, as illustrated in Fig. 7.

3.2. Data analysis

Data were analyzed using the methods described in Experiment 1. To reduce the variance in pupil size across different recordings, the pupil size was calculated from the eye images and reported relative to the size of the iris. For each of the 500 images recorded during the fixation task, five images were selected at random. Iris and pupil borders were manually extracted from the selected images, and the pupil size was taken as the average horizontal pupil diameter divided by the average diameter of the iris.

Table 6
Summary of saccade properties with a maximally a_{max} and minimally a_{min} accommodated lens at the far viewing distance. $\hat{\varphi}$ represents the normalized pupil size, defined as the horizontal pupil diameter divided by the horizontal diameter of the iris.

Part.	Cond.	No.	PV (M ± SD)	A_{PSO} (M ± SD)	$A_{PSO}^{P_1}$ (M ± SD)	$\hat{\varphi}$
IH	a_{max}	81	274.86 ± 28.55	0.35 ± 0.22	0.12 ± 0.11	0.11
IH	a_{min}	87	268.95 ± 31.15	0.19 ± 0.15	0.13 ± 0.11	0.54
TC	a_{max}	66	280.12 ± 37.04	0.28 ± 0.15	0.12 ± 0.11	0.18
TC	a_{min}	66	278.99 ± 18.31	0.67 ± 0.21	0.16 ± 0.11	0.62
RA	a_{max}	65	323.56 ± 43.41	0.89 ± 0.27	0.14 ± 0.10	0.13
RA	a_{min}	61	373.33 ± 33.04	1.43 ± 0.35	0.13 ± 0.09	0.67
MN	a_{max}	102	363.24 ± 38.93	0.92 ± 0.23	0.23 ± 0.19	0.18
MN	a_{min}	100	390.65 ± 22.94	1.72 ± 0.54	0.29 ± 0.16	0.66

3.3. Results

Saccade properties are summarized in Table 6. Fig. 8 illustrates the effect of lens accommodation on PSOs for participant RA. In contrast to Fig. 4 in Experiment 1, a pharmacologically induced lens accommodation produced smaller PSO-amplitudes compared to when the lens accommodation was reduced. The effect of treatment on PSOs is further illustrated in Fig. 9. As can be seen from the figure, a high degree of lens accommodation does generally not lead to larger PSOs compared to a low degree of lens accommodation (max accom: 0.62 ± 0.37, min accom: 1.04 ± 0.75). On the contrary, none of the participants had their largest PSOs in the accommodated state, and the PSO amplitude decreased on average by 40% when the lens was in the accommodated state compared to the non-accommodated state. As seen in Table 7, PSO-amplitudes were the smallest in the control condition (no treatment), but the differences between treatments were not significant. Furthermore, three of the participants (TC, $t(45) = -8.34$, $p < 0.01$; RA, $t(47) = -9.34$, $p < 0.01$; MN, $t(73) = -14.98$, $p < 0.01$) had their largest PSO-amplitudes when lens accommodation was reduced.

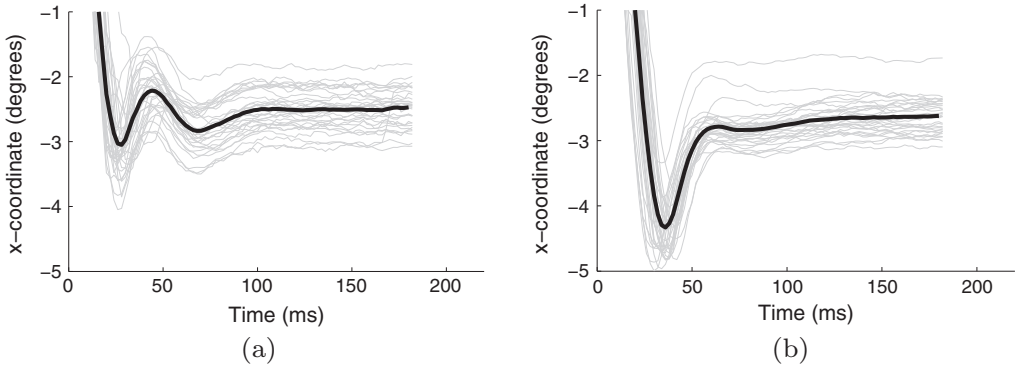

Fig. 8. PSO-trajectories for five-degree saccades with a maximally (a) and minimally (b) accommodated lens. The data show leftward saccades performed by participant RA. All saccades were recorded at the far viewing distance, i.e., 70 cm.

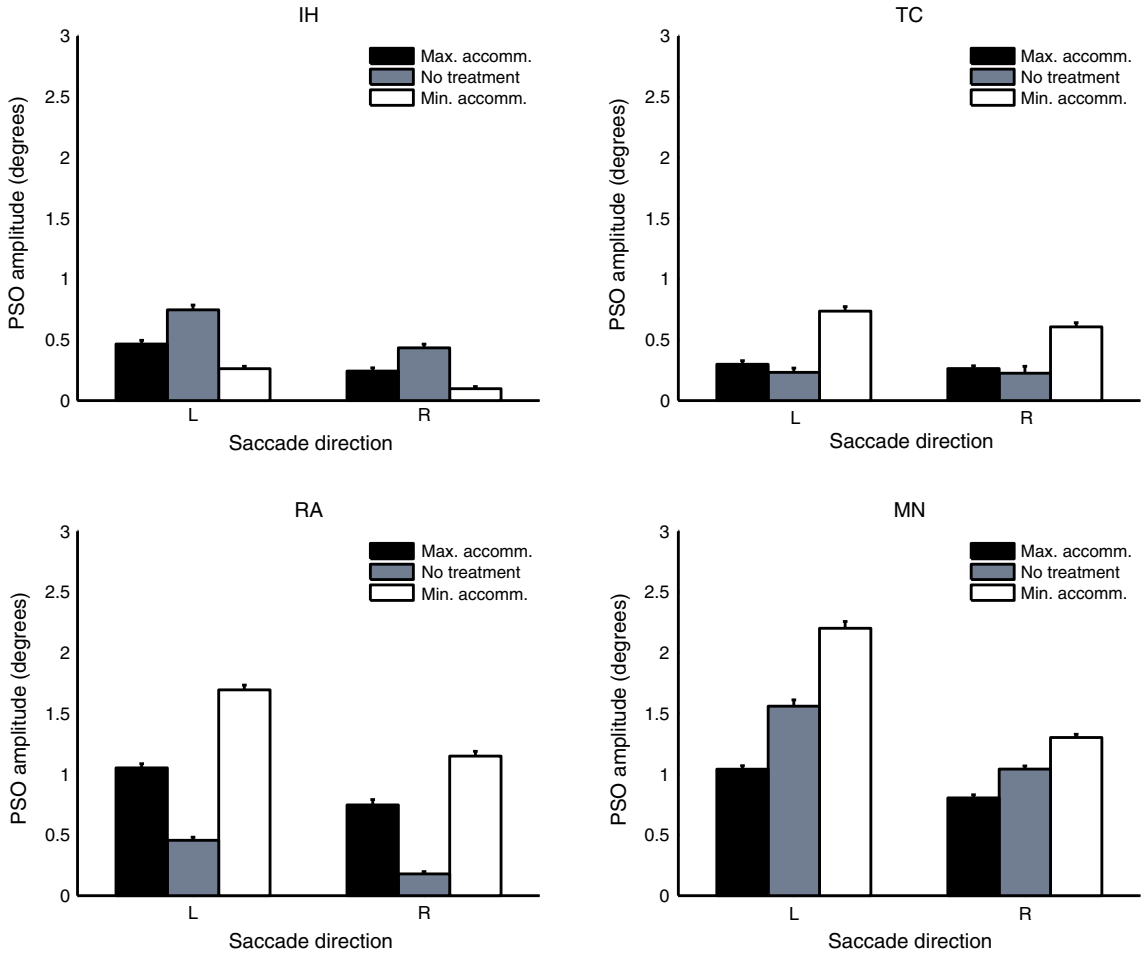

Fig. 9. Effect of pharmacological lens accommodation on PSO-amplitude. The viewing distance was 70 cm during all recordings. Data from Experiment 1 (No Treatment) are included for comparison.

Table 7
Results of the linear mixed effects model when **PSO-amplitude** is predicted by the treatments (no treatment, maximum accommodation and minimum accommodation).

	Estimate	Std. error	*t* value
(Intercept)	0.74	0.12	6.29
Max accom.	0.02	0.13	0.14
Min accom.	0.20	0.21	0.95

One of the participants, IH, had larger PSO-amplitudes when the lens was in its accommodated state compared to the non-accommodated state. For this participant, however, both treatments resulted in small PSO-amplitudes, both with respect to absolute numbers and compared to the control condition (no treatment).

Fig. 10 shows the effect the eye drops have on the P_1 signal. On average, PSO amplitudes of the P_1-signal were larger in the

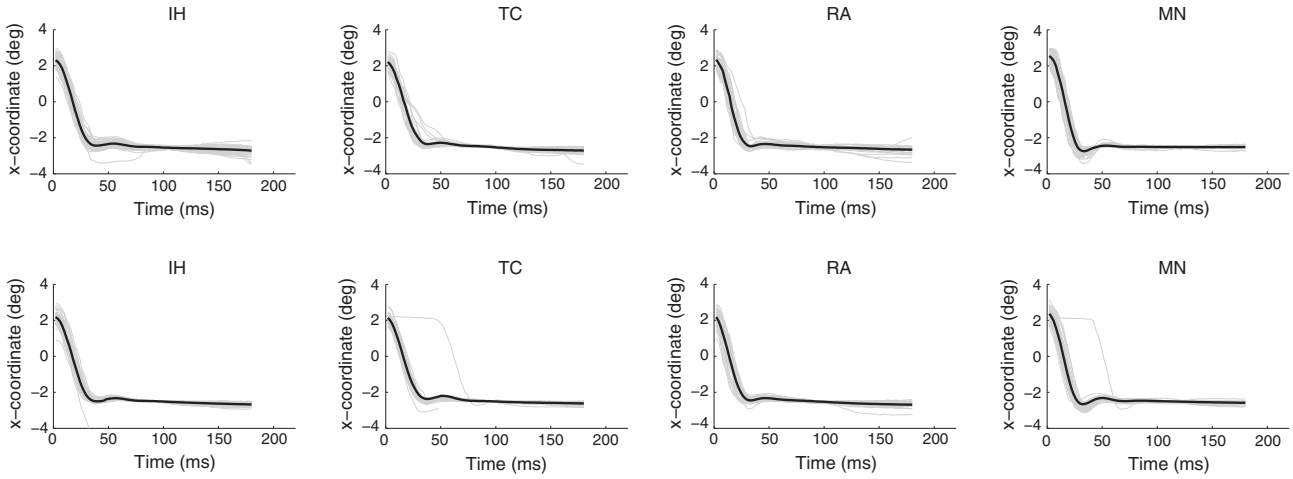

Fig. 10. The first Purkinje image (P_1)-signal with a maximally (upper panel) and minimally (lower panel) accommodated lens. The signals originate from leftward saccades conducted at the 'far' viewing distance. To facilitate comparisons between the figures, the signals have been converted to degrees and centered around zero on the *y*-axis.

Table 8
Results of the linear mixed effects model when **PSO-amplitude of the P_1-signal** is predicted by the treatments (no treatment, maximum accommodation and minimum accommodation). Significance is indicated by '*'.

	Estimate	Std. error	*t* value
(Intercept)	0.34	0.03	10.87
Max accom.	0.01	0.02	0.54
Min accom.	0.05	0.02	2.48*

non-accommodated state compared to the accommodated state (min. accommodation: 0.19 ± 0.14 deg., max. accommodation: 0.16 ± 0.15 deg.). While the former were not significantly different from each other, P_1-amplitudes in the non-accommodated state were significantly larger than those in the control condition (0.15 ± 0.13 deg., see Table 8).

3.4. Discussion

A pharmacologically induced lens accommodation did overall not lead to larger PSO amplitudes compared to when the accommodation was reduced. Consequently, this result does not support the lens–pupil hypothesis. Importantly, the rotation of the eyeball, estimated by the P_1, was largely unaffected by the pharmacological manipulation (average differences less than 0.04 deg.), and is therefore omitted from analyzes in the following experiments. Since an increase in PSO amplitude was found in Experiment 1, where viewing distance was used to manipulate lens accommodation, we investigate in Experiment 2b whether the vergence angle could mediate the relationship between the lens- and the pupil oscillations. According to the lens–pupil hypothesis, we expect no or small differences in PSO-amplitude during the pharmacological manipulations since the lens accommodation remains constant between the near and far conditions. Hence, any observed difference is likely to be attributed to the change in vergence angle and/or other factors associated with this change.

4. Experiment 2b

4.1. Participants, materials, and procedure

The participants and experimental setup were the same as during the first two experiments. In this experiment, we also recorded eye movements with pharmacologically manipulated lens accommodation in the near-condition, i.e., a viewing distance at 17 cm.

Table 9
Summary of saccade properties with a maximally a_{max} and minimally a_{min} accommodated lens at the near viewing distance. $\hat{\varphi}$ represents the normalized pupil size, defined as the horizontal pupil diameter divided by the horizontal diameter of the iris.

Part.	Cond.	No.	PV (M ± SD)	A_{PSO} (M ± SD)	$\hat{\varphi}$
IH	a_{max}	85	299.32 ± 40.91	0.95 ± 0.32	0.11
IH	a_{min}	62	298.02 ± 40.27	0.46 ± 0.24	0.54
TC	a_{max}	53	306.39 ± 22.62	0.89 ± 0.24	0.15
TC	a_{min}	7	293.31 ± 29.86	0.87 ± 0.11	0.63
RA	a_{max}	29	395.93 ± 46.62	1.61 ± 0.26	0.13
RA	a_{min}	48	407.33 ± 38.39	1.93 ± 0.48	0.66
MN	a_{max}	112	391.44 ± 61.07	1.41 ± 0.46	0.17
MN	a_{min}	43	384.09 ± 36.53	1.83 ± 0.58	0.65

4.2. Results

A summary of the saccade properties at the near viewing condition is presented in Table 9.

Saccade trajectories from participant RA with a pharmacologically reduced lens accommodation can be seen in Fig. 11. The figure shows that PSO-amplitudes at near are about 0.5 deg. larger than at far. Fig. 12 illustrates how the PSO-amplitude differs between near and far for both treatments. Differences from Experiment 1 are included for comparison. The figure shows that irrespective of whether the accommodative state of the lens is at its maximum (near: 1.19 ± 0.46 deg., far: 0.63 ± 0.37 deg.) or minimum (near: 1.29 ± 0.8 deg., far: 1.02 ± 0.74 deg.), PSO-amplitudes are systematically larger in the near condition. This observation is verified statistically in Table 10. PSO-amplitudes were significantly larger at near also when each participant's data were analyzed separately (all $p < 0.01$).

Furthermore, differences in PSO-amplitudes between near and far were the largest in the control condition followed by the accommodated state, and finally the non-accommodated state of lens accommodation. There was a significant difference only between the control condition and when the lens accommodation was at its reduced state, as can be seen in Table 11.

4.3. Discussion

The PSO-amplitude increased at the near compared to the far condition, irrespective of the accommodative state of the lens. This provides further evidence that lens oscillation does not fully explain PSOs observed in signals recorded with pupil-based eye trackers. Instead, other factors associated with the change in vergence angle and/or other effects related to this change are likely to significantly influence the amplitude of PSOs. However, that

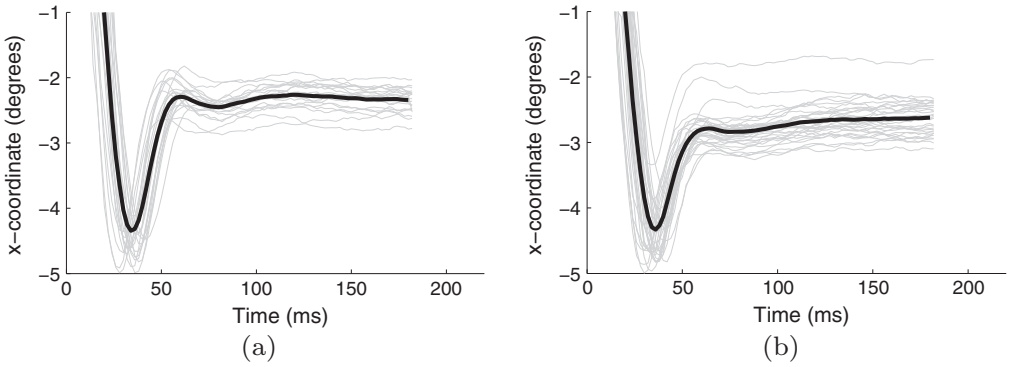

Fig. 11. PSO-trajectories for five-degree saccades with a minimally accommodated lens at near (a) an far (b). The data show leftward saccades performed by participant RA.

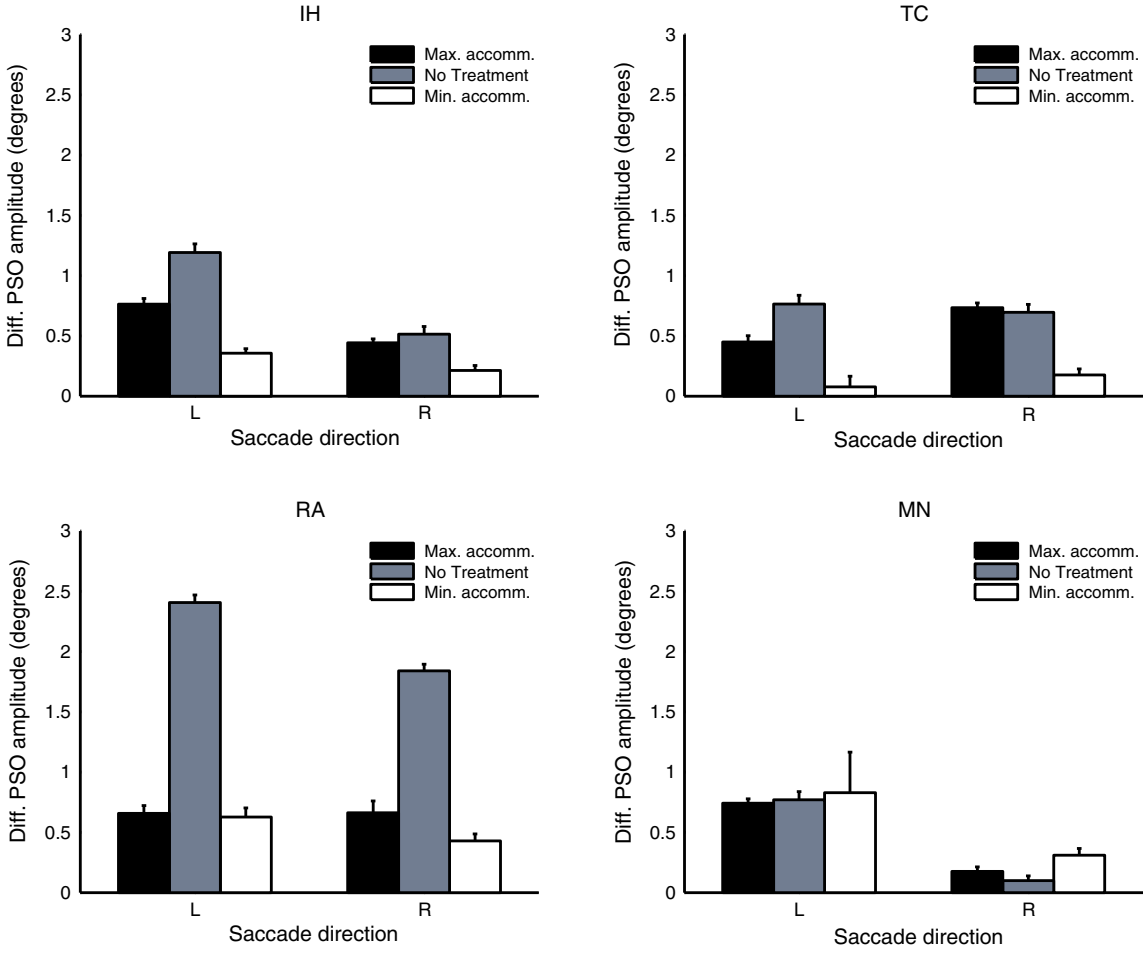

Fig. 12. Difference in PSO-amplitude between near and far viewing conditions. A positive values means that PSO-amplitudes at near are larger than those at far. Results from Experiment 1 (No Treatment) are included for comparison.

Table 10
Results of the linear mixed effects model when **PSO-amplitude** is predicted by viewing condition (near/far) while pharmacologically keeping the lens accommodation fixed in a maximally or minimally accommodated state. Significance is indicated by '*'.

	Estimate	Std. error	*t* value
(Intercept)	0.74	0.12	6.27
Near	0.34	0.05	7.29*
Min accom.	0.18	0.12	1.52
Near:min accom.	−0.19	0.05	−4.07*

Table 11
Results of the linear mixed effects model when difference in **PSO-amplitude** between near and far is predicted by the treatments (no treatment, maximum accommodation and minimum accommodation). Significance is indicated by '*'.

	Estimate	Std. error	*t* value
(Intercept)	0.74	0.12	6.29
Max accom.	−0.45	0.32	−1.38
Min accom.	−0.95	0.22	−4.35*

the control condition (no treatment) produced the largest differences in PSO-amplitudes also suggests that the eye drops keep some dynamic properties of the eye relatively constant across the viewing conditions.

5. Experiment 3

Besides affecting the shape of the lens, the eye drops used in this study also influence the size of the pupil; Isopto–Pilokarpin constrict the pupil and Cyclopentolat dilates the pupil. In an attempt to separate the effects of lens accommodation and pupil size on PSO, an experiment is conducted where the pupil size was manipulated by changes in brightness.

5.1. Participants, materials, and procedure

Four participants participated in the experiment. Two of the participants, MN and RA, also participated in the previous experiments. The other two were HG (age: 52 years, gender: m) and CL (37, f) The apparatus and experimental setup were the same as during the first two experiments. Eye movements were recorded at the 'far' distance (70 cm) in two conditions: in a bright environment (183 LUX at the position of the eye) with the stimulus consisting of a white background and gray dots and a dark environment (<1 LUX) where the stimulus background was changed to black.

5.2. Results

The pupil size and PSO-parameters were extracted as described in the previous experiments. Data on how the pupil was affected

Table 12
Summary of saccade properties with a small a_{max} and large a_{min} pupil size at the far viewing distance. $\hat{\varphi}$ represents the normalized pupil size, defined as the horizontal pupil diameter divided by the horizontal diameter of the iris.

Part.	Cond.	No.	PV (M ± SD)	A_{PSO} (M ± SD)	$\hat{\varphi}$
HG	Bright	47	342.20 ± 34.43	0.56 ± 0.26	0.21
HG	Dark	65	350.85 ± 53.10	0.79 ± 0.25	0.55
CL	Bright	71	301.85 ± 23.29	0.84 ± 0.51	0.25
CL	Dark	67	302.21 ± 27.34	0.93 ± 0.37	0.54
RA	Bright	78	305.17 ± 41.32	0.26 ± 0.16	0.23
RA	Dark	53	338.98 ± 40.55	0.45 ± 0.32	0.57
MN	Bright	98	321.49 ± 36.37	0.68 ± 0.38	0.24
MN	Dark	87	354.98 ± 38.40	0.88 ± 0.41	0.54

by the changes in brightness as well as how the change in pupil size influences PSOs are provided in Table 12. A set of saccade trajectories from participant RA is shown in Fig. 13. In RA's case, the PSO-amplitude becomes almost twice as large when saccades are conducted in darkness and the pupil is large. Across all participants, there was a significant effect of viewing condition on PSO amplitude, which increased by 18% in the dark condition (dark: 0.85 ± 0.25 deg., bright: 0.72 ± 0.27 deg., see Table 13). When analyzed individually, all participants besides CL (dark: 0.93 ± 0.37 deg., bright: 0.84 ± 0.51 deg., $t(66) = 1.92, p = 0.08$) had significantly larger PSO amplitudes in the 'dark' condition. PSO-amplitudes for all participants are shown in Fig. 14, divided into abducting and adducting saccades.

5.3. Discussion

PSO amplitudes became on average 18% higher when recorded in darkness with a large pupil size. While an attempt was made to isolate the effect of pupil size on PSO amplitude, it should be noted that other factors part of the accommodative response such as lens shape may also have been affected. A complete separation of pupil size and lens accommodation is difficult (impossible?) to implement. Moreover, the increase in pupil size from the bright to the dark condition was smaller than the difference caused by the eye drops (a factor 2.38 versus a factor 4.5), suggesting that the contribution of pupil size in Experiment 2 may be even larger than reported here. In summary, these results suggest that pupil size may by an important factor to take into consideration when investigating post-saccadic portions of the eye-tracker signal.

6. Experiment 4

Another potential factor that could affect PSO is that fact that a three-dimensional (3D) object, the eye, is projected onto a 2D surface, the camera sensor. When the eye is observed from an oblique angle, the pupil shape changes its appearance in the eye image. In this experiment, a practical approach is taken to address this question by recording saccades of the same size for different angles of the eye relative to the camera.

Table 13
Results of the linear mixed effect model when predicting PSO-amplitude from viewing condition (dark and bright). The table shows that **PSO-amplitudes** in the dark condition are significantly larger ($t > 2$) than those in the bright condition. Significance is indicated by '*'. Notice that the PSO-amplitudes are log transformed before being used in the model.

	Estimate	Std. error	t value
(Intercept)	0.72	0.09	8.43
Dark	0.11	0.02	5.13*

6.1. Participants, materials, and procedure

The same participants, instructions, and experimental setup were used as in Experiment 3. Five degree saccades were conducted as described in the previous experiment between white targets presented on a dark background. The targets were presented at positions $((-2.5, 0), (2.5, 0)), ((-12.5, 0), (-7.5, 0))$, and $((7.5, 0), (12.5, 0))$ deg. Each of the three pairs of targets was displayed for 60 s. Between each presentation there was a three second pause where participants were asked to blink.

6.2. Results

Saccade trajectories from participant RA are shown in Fig. 15. Even though differences in PSO-amplitudes can be observed within participants, they are generally small and unsystematic (Fig. 16). On average, PSO amplitudes are not significantly different across the different eye orientations (−10 deg.: 0.98 ± 0.27, 0 deg.: 0.95 ± 0.27, 10 deg.: 0.95 ± 0.31, see Table 15). More detailed information about the saccades divided into participants and conditions can be found in Table 14.

6.3. Discussion

Like the influence of dynamic overshoot of the eyeball on PSOs, the gaze direction seems to have negligible effects on PSO-shapes and amplitudes over the tested 20 deg. of the visual field. Future, more detailed investigations of PSOs in relation to eye-camera angles should ideally present targets on an iso-vergence screen and consider individual variation in pupillary distance.

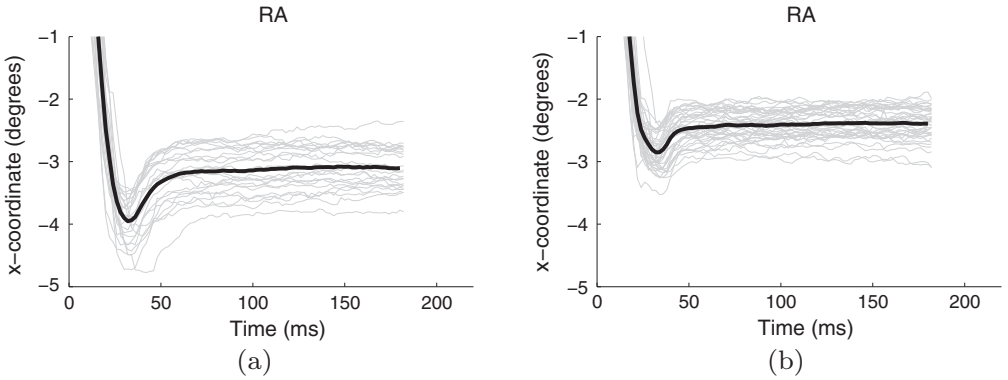

Fig. 13. PSO-trajectories for five-degree saccades conducted in a dark (a) and a bright (b) environment, affecting the pupil size. The data show leftward saccades performed by participant RA.

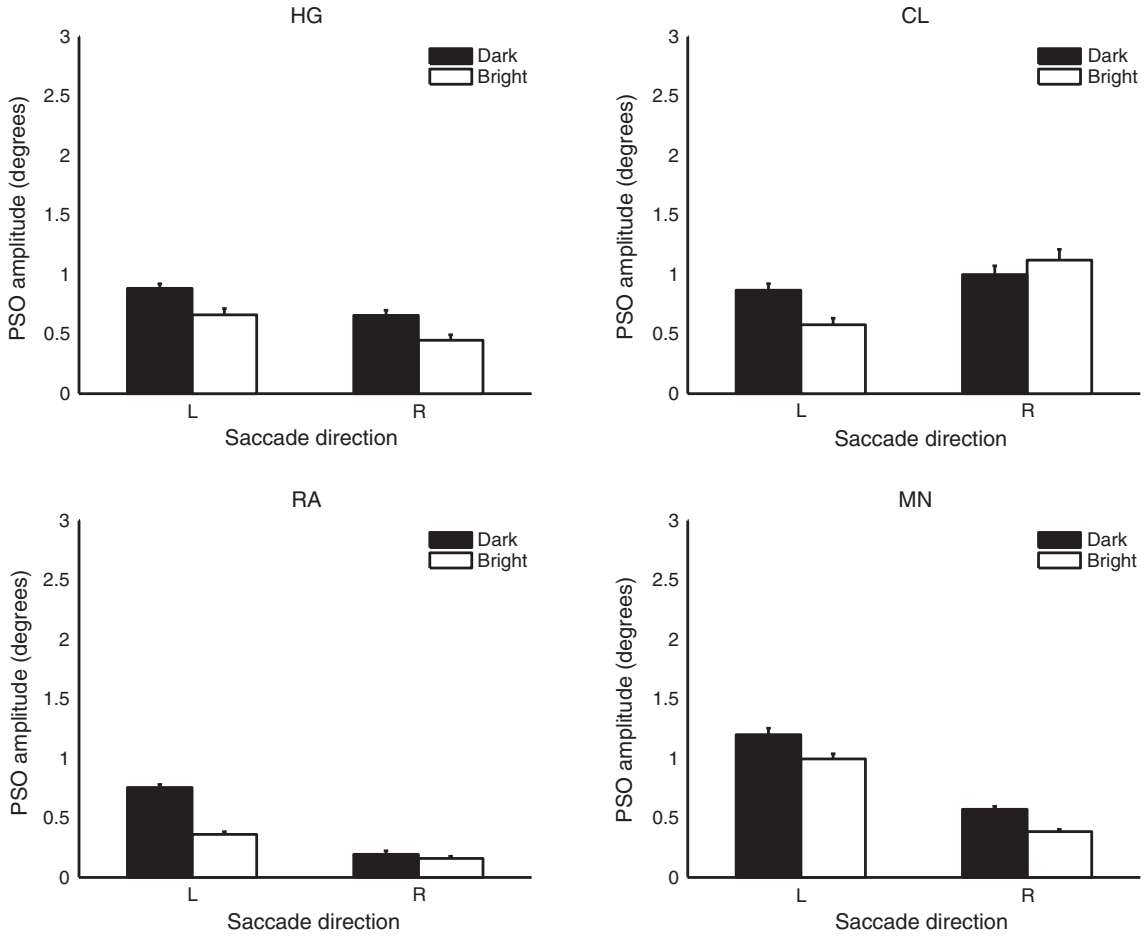

Fig. 14. PSO-amplitude for large and small pupil sizes.

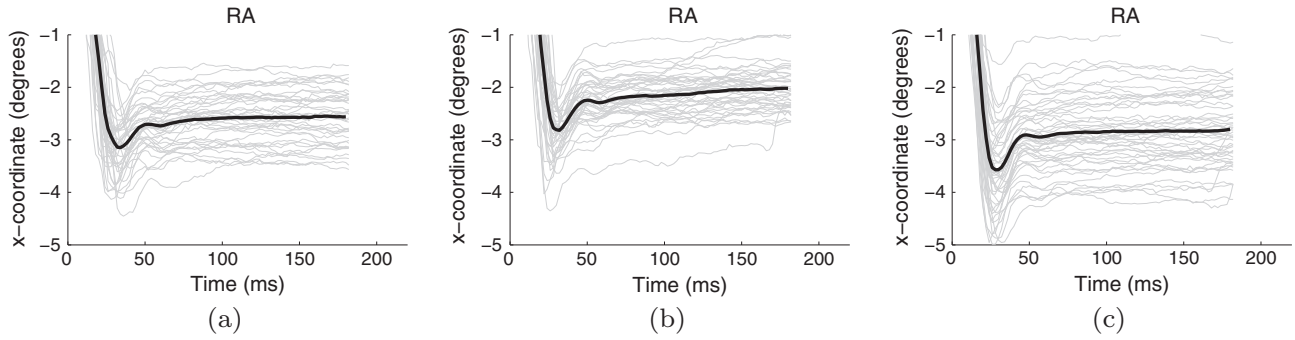

Fig. 15. PSO-trajectories for five-degree saccades centered at (a) −10 deg. (b) 0 deg., and (c) 10 deg. The data show leftward saccades performed by participant RA.

7. General discussion

Post-saccadic oscillations are commonly seen in eye-tracker data due to lens and pupil oscillations immediately following saccades. In this paper we investigated the pupil–lens hypothesis, i.e., that PSOs in pupil-based eye trackers occur mainly as a consequence of lens wobbles, which we know from previous studies increase at near compared to far accommodation (He et al., 2010). In four experiments, PSO-amplitude was measured in response to manipulations of lens accommodation and the potential confounds pupil size and eye orientation.

In the first experiment, we replicated and extended the results by Hutton (2013) showing that saccade peak velocities increase and PSOs have larger amplitudes at near compared to far accommodation. Based on these data we cannot reject the hypothesis that lens wobble is a source of PSOs in pupil-based eye trackers. In addition, we observed an abducting/adducting asymmetry with respect to saccade peak velocity and PSO amplitude, similar to that found with scleral search coils (Kapoula, Robinson & Hain, 1986) and DPIs (He et al., 2010).

In Experiment 2a, we manipulated lens accommodation pharmacologically and had participants conduct saccades identical to the far condition in Experiment 1 (i.e., at 70 cm). According to the lens–pupil hypothesis, we expected the pharmacological manipulation leading to a maximally accommodated lens to produce larger saccade peak velocities and the largest-amplitude

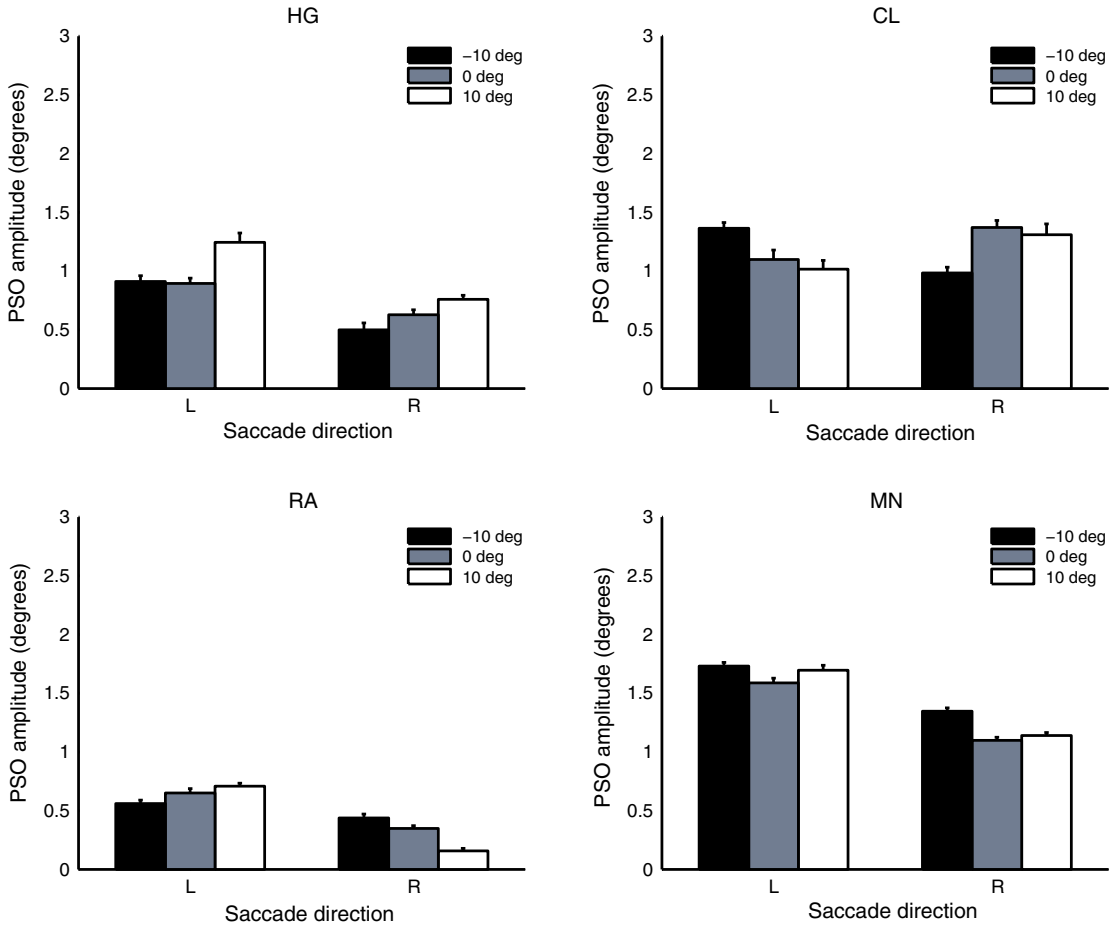

Fig. 16. PSO-amplitudes for three different gaze directions.

Table 14
Summary of saccade properties for different eye orientations.

Part.	Cond. (deg.)	No.	PV (M ± SD)	A_{PSO} (M ± SD)
HG	−10	59	361.11 ± 58.83	0.73 ± 0.35
HG	0	63	335.35 ± 39.70	0.78 ± 0.28
HG	10	70	343.72 ± 46.46	1.00 ± 0.43
CL	−10	70	349.96 ± 24.48	1.22 ± 0.35
CL	0	57	340.68 ± 21.92	1.24 ± 0.40
CL	10	46	347.07 ± 28.88	1.16 ± 0.42
RA	−10	78	326.76 ± 29.42	0.50 ± 0.20
RA	0	82	335.79 ± 45.23	0.50 ± 0.25
RA	10	88	323.48 ± 58.68	0.45 ± 0.32
MN	−10	93	532.20 ± 57.51	1.54 ± 0.28
MN	0	97	509.62 ± 60.54	1.36 ± 0.35
MN	10	96	504.37 ± 74.03	1.43 ± 0.37

Table 15
Results of the linear mixed effect model when predicting **PSO-amplitude** from eye orientation. The eye orientation 0 deg. is used as baseline in the model. Notice that the PSO-amplitudes are log transformed before being used in the model.

	Estimate	Std. error	*t* value
(Intercept)	0.95	0.11	8.81
−10 deg.	0.01	0.03	0.53
10 deg.	0.01	0.04	0.29

PSO and vice versa. However, we found no overall support for this in the data. If anything, there was a distinct trend in the opposite direction for three of the participants. Consequently, these result do not provide any support of the lens–pupil hypothesis.

In Experiment 2b, the vergence angle was manipulated while keeping the degree of accommodation pharmacologically fixed (maximized or minimized). Overall, PSO-amplitudes at large vergence angles (near) were larger than those at small vergence angles (far). Consequently, a large degree of the increase in PSO-amplitude at near in Experiment 1 can be explained by a change in vergence angle and any associated effect of this change, rather than pupil oscillations induced by the increase in lens accommodation. Taken together, the results from Experiments 1, 2a, and 2b do not support the lens–pupil hypothesis, which predicts that lens wobble is a main source of PSOs in pupil-based eye trackers.

Irrespective of whether a model including lens wobble or fluid friction best accounts for PSOs in pupil based eye trackers, we know that PSO-amplitude is highly correlated with peak velocity (Experiment 1) and peak deceleration of the saccade (Kimmel, Mammo & Newsome, 2012). A superordinate explanation to why PSO-amplitudes are larger at near would therefore be if dynamic overshoot of the eyeball increased at the near viewing distance, something that would (fully or in part) account for the larger PSO-amplitude found by Hutton (2013) and in Experiment 1. This explanation was addressed by measuring whether the P_1, representing motion of the eyeball, was influenced by viewing distance (Experiment 1) and the pharmacological manipulations (Experiment 2a). In agreement with Schachar et al. (2007) who tracked the P_1 using a DPI eye tracker, we found a significant but in absolute terms small increase in PSO-amplitude of the P_1-signal at near.

While Schachar et al. (2007) observed a 0.04 deg. difference between near (15 cm, 0.09 deg.) and far (70 cm, 0.05 deg.), we reported a difference of 0.12 deg. (near: 0.26 deg., far: 0.14). One possible explanation for the difference between the results by Schachar et al. (2007) and those in this paper is the higher precision of the P_1-signal acquired with the DPI. Regarding the effect of pharmacological treatment on PSO in the P_1-signal, the effects were also small with difference less than 0.04 deg. Based on these finding, we conclude that while eyeball rotation contributes to PSOs in the eye-tracker signal, its relative influence is minor.

The eye drops used in the study, Pilokarpin and Cyklopentolat, do not affect lens accommodation in isolation; Isopto-Pilocarpine (2%) is a cholinergic drug that stimulates (muscarinic agonist) receptors on smooth muscles in the eye. This induces contraction of the m. ciliaris and m. sphincter pupillae. Cyclopentolat (1%) is an anticholinergic drug (muscarinic antagonist) that prevents contraction of the same muscles. The most common side effects of the drugs are blurry vision and changes in light sensitivity. These effects are well documented and a logical consequence of the affected accommodation and change in pupil size. If there are any other side effects of the formulas that influences the lens suspension or iris structure is to our knowledge not known. This could theoretically change the dynamics of PSOs, inducing confounding factors in the experimental design.

In Experiment 3, the most distinct effect of the drugs besides the lens accommodation—the change in pupil size—was investigated. On average, the PSO-amplitude increased by 18% when the pupil size was large (55% of the iris) compare to small (23% of the iris), a change of a factor 2.4 in pupil size. These results should be seen in relation to the factor 4.42 change in pupil size due to the pharmacological treatments (Experiment 2a, large: 62%, small: 14%) which led to an increase in PSO-amplitude of 67% (PSO-amplitude large pupil size/min accommodation: 1.04 deg., PSO-amplitude small pupil size/max accommodation: 0.62 deg.). One could therefore speculate that part the increase in PSO-amplitude in Experiment 2a is due to the increase in pupil size rather than related to the accommodative state of the lens. Future manipulations that better separate changes in pupil size from lens accommodation are probably required to provide a more fine-grained answer to this question.

During version or vergence eye movements, the angle between the eye and the camera typically changes. As an effect the pupil is being filmed from different perspectives and the shape of the pupil in the video image changes. In Experiment 4, the influence of such changes on PSOs was investigated by having participants conduct saccades at different eye orientations. The central 20 degree region, where the majority of saccades are conducted in typical screen-based experiments, was tested. Overall, we found no systematic differences in PSO-amplitude based on gaze direction within this range and conclude that eye orientation under normal experimental conditions is not a main factor that affects PSOs. It should be noted that a more theoretical approach to investigate the effect of eye-camera angles on PSOs could involve ray tracing (see, e.g., He et al., 2010).

Alternative mechanisms behind PSOs have been proposed in research investigating the effect of intra-ocular lenses (IOL) on post-saccadic instability of the eye. Jacobi and Jagger (1981) emphasize the contribution of eyeball fluids to oscillations in the iris, known as 'iridodonesis'. Specifically, they argue that since the eye is non-rigid, one would expect part of the kinetic energy from saccadic eye movements to be dissipated through fluid friction. They propose that when the eyeball starts to accelerate during a saccade, the aqueous stays behind the eyeball due to inertia, and for the same reason oscillates at the end of the saccade. Jacobi and Jagger (1981) further propose that the oscillation can be modeled as a damped harmonic oscillation where the aqueous comprise the mass, the iris stroma the spring, and the damping is due to fluid friction. The model is used to explain why two different methods to insert IOLs generate different amounts of post-saccadic IOL-wobbles.

In the ophthalmological domain, it is well known that the absence of a lens gives rise to iridodonesis. This is since, under normal condition, the lens and its capsule comprise a stabilizing barrier against fluid oscillation in the aqueous and vitreous cavity (Srivastava, Vasavada & Vasavada, 2012). Due to the importance of eyeball fluids and their visco-elastic properties on post-saccadic oscillations in various ocular structures, it may be too simple to explain PSOs in pupil based eye trackers as a direct result of lens wobbles. Instead, a fluid based origin of PSOs suggests more complicated, multifaceted explanations to why and when we would expect to see oscillations of the pupil.

In light of the findings and the reviewed literature in this paper, it seems as if there is no simple model that can fully describe PSOs in pupil-based eye trackers. In a wider perspective, only five degree saccades have been tested in this paper. It is well known that the dynamics of larger-amplitude saccades changes (Collewijn, Erkelens & Steinman, 1988), which raises the question of whether these results can be generalized over a wider spectrum of saccade amplitudes.

It is clear from the findings in this paper that differences in saccade shapes and PSOs can be large depending on the situation under which they are recorded. In practice, this means that basic measures in eye movement research such as saccade peak velocity, saccade amplitude, and fixation duration also may vary. One way to deal with this uncertainty is to explicitly take PSOs into account when detecting, e.g., fixation and saccade events. Such event detection algorithms have for instance been proposed by Nyström and Holmqvist (2010) and Larsson, Nyström and Stridh (2013).

8. Conclusions

Through experimental and pharmacological manipulations of crystalline lens accommodation, we tested the lens–pupil hypothesis, i.e., that post-saccadic oscillations (PSOs) in pupil based eye trackers primarily are caused post-saccadic wobbling of the lens. While we could replicate previous research showing that PSO-amplitudes increase at near viewing distances, when the lens is in an accommodated state, the effect was absent when pharmacologically manipulating lens accommodation at a fixed viewing distance. In summary, we rejected the lens–pupil hypothesis as well as tested and discussed alternative explanations to why PSOs occur in eye-tracker data recorded from pupil-based systems. Simultaneous recording of several eye structures during the same saccade would provide important information about the components a successful model that accounts for PSOs should include.

Acknowledgments

The reviewers are acknowledged for valuable comments. In particular, we thank one of the reviewers for comments that led to Experiments 3 and 4. The experiments were conducted in the Lund University Humanities Laboratory, Lund, Sweden.

References

Bates, D., Maechler, M., Bolker, B., & Walker, S. (2013). *lme4: Linear mixed-effects models using Eigen and S4*. R package version 1.0-4.

Collewijn, H., Erkelens, C. J., & Steinman, R. (1988). Binocular co-ordination of human horizontal saccadic eye movements. *The Journal of Physiology, 404*, 157–182.

Crane, H., & Steele, C. (1985). Generation-v dual-purkinje-image eyetracker. *Applied Optics, 24*, 527–537.

Deubel, H., & Bridgeman, B. (1995a). Fourth purkinje image signals reveal eye-lens deviations and retinal image distortions during saccades. *Vision Research, 35*, 529–538.

Deubel, H., & Bridgeman, B. (1995b). Perceptual consequences of ocular lens overshoot during saccadic eye movements. *Vision Research, 35*, 2897–2902.

Engbert, R., & Kliegl, R. (2003). Microsaccades uncover the orientation of covert attention. *Vision Research, 43*, 1035–1045.

Glasser, A., & Kaufman, P. L. (1999). The mechanism of accommodation in primates. *Ophthalmology, 106*, 863–872.

He, L., Donnelly, W., III, Stevenson, S., & Glasser, A. (2010). Saccadic lens instability increases with accommodative stimulus in presbyopes. *Journal of Vision, 10*.

Hooge, I., Nyström, M., Cornelissen, T., & Holmqvist, K. (2013). Properties of post-saccadic oscillations induced by eye trackers. In K. Holmqvist, F. Mulvey, & R. Johansson (Eds.), *Book of abstracts of the 17th european conference on eye movements* (Vol. 6). Lund, Sweden.

Hutton, S. (2013). Lens mobility influences post-saccadic ringing in video-based eye tracking. In K. Holmqvist, F. Mulvey, & R. Johansson (Eds.), *Book of abstracts of the 17th European conference on eye movements* (Vol. 6). Lund, Sweden.

Jacobi, K. W., & Jagger, W. S. (1981). Physical forces involved in pseudophacodonesis and iridodonesis. *Albrecht von Graefes Archiv für klinische und experimentelle Ophthalmologie, 216*, 49–53.

Kapoula, Z., Robinson, D., & Hain, T. (1986). Motion of the eye immediately after a saccade. *Experimental Brain Research, 61*, 386–394.

Kimmel, D., Mammo, D., & Newsome, W. (2012). Tracking the eye non-invasively: Simultaneous comparison of the scleral search coil and optical tracking techniques in the macaque monkey. *Frontiers in Behavioral Neuroscience, 6*.

Larsson, L., Nyström, M., & Stridh, M. (2013). Detection of saccades and post-saccadic oscillations in the presence of smooth pursuit. *IEEE Transactions on Biomedical Engineering, 60*, 2484–2493.

Leigh, R. J., & Zee, D. S. (2006). *The neurology of eye movements* (4th ed.). New York, NY: Oxford University Press.

Nyström, M., & Holmqvist, K. (2010). An adaptive algorithm for fixation, saccade, and glissade detection in eye-tracking data. *Behavior Research Methods, 42*, 188–204.

Nyström, M., Hooge, I., & Holmqvist, K. (2013). Post-saccadic oscillations in eye movement data recorded with pupil-based eye trackers reflect motion of the pupil inside the iris. *Vision Research, 92*, 59–66.

Rang, H., Dale, M. M., Ritter, J., & Moore, P. (2003). *Pharmacology* (5th ed.). Edinburgh: Churchill Livingstone.

R Core Team (2013). *R: A language and environment for statistical computing*. Austria: R Foundation for Statistical Computing Vienna.

Schachar, R. A., Davila, C., Pierscionek, B. K., Chen, W., & Ward, W. W. (2007). The effect of human in vivo accommodation on crystalline lens stability. *British Journal of Ophthalmology, 91*, 790–793.

Srivastava, S., Vasavada, V. A., & Vasavada, V. A. (2012). High-speed imaging of the glued IOL. In V. A. Vasavada (Ed.), *Glued IOL: Glued intrascleral haptic fixation of a PC IOL* (pp. 175–178). New Delhi, India: Jaypee Brothers Medical Pub.